

NACA RM L51D16



~~NACA~~

RESEARCH MEMORANDUM

A FLIGHT INVESTIGATION OF THE DAMPING IN ROLL AND
ROLLING EFFECTIVENESS INCLUDING AEROELASTIC EFFECTS OF
ROCKET-PROPELLED MISSILE MODELS HAVING CRUCIFORM,
TRIANGULAR, INTERDIGITATED WINGS AND TAILS

By Russell N. Hopko

Langley Aeronautical Laboratory
Langley Field, Va.

UNCLASSIFIED
Placed into Hopko doc 8/10/52
Good, please making use of 67 (a) (1) (b) (1) (c) (1) (d) (1) (e) (1) (f) (1) (g) (1) (h) (1) (i) (1) (j) (1) (k) (1) (l) (1) (m) (1) (n) (1) (o) (1) (p) (1) (q) (1) (r) (1) (s) (1) (t) (1) (u) (1) (v) (1) (w) (1) (x) (1) (y) (1) (z) (1) (aa) (1) (ab) (1) (ac) (1) (ad) (1) (ae) (1) (af) (1) (ag) (1) (ah) (1) (ai) (1) (aj) (1) (ak) (1) (al) (1) (am) (1) (an) (1) (ao) (1) (ap) (1) (aq) (1) (ar) (1) (as) (1) (at) (1) (au) (1) (av) (1) (aw) (1) (ax) (1) (ay) (1) (az) (1) (ba) (1) (bb) (1) (bc) (1) (bd) (1) (be) (1) (bf) (1) (bg) (1) (bh) (1) (bi) (1) (bj) (1) (bk) (1) (bl) (1) (bm) (1) (bn) (1) (bo) (1) (bp) (1) (bq) (1) (br) (1) (bs) (1) (bt) (1) (bu) (1) (bv) (1) (bw) (1) (bx) (1) (by) (1) (bz) (1) (ca) (1) (cb) (1) (cc) (1) (cd) (1) (ce) (1) (cf) (1) (cg) (1) (ch) (1) (ci) (1) (cj) (1) (ck) (1) (cl) (1) (cm) (1) (cn) (1) (co) (1) (cp) (1) (cq) (1) (cr) (1) (cs) (1) (ct) (1) (cu) (1) (cv) (1) (cw) (1) (cx) (1) (cy) (1) (cz) (1) (da) (1) (db) (1) (dc) (1) (dd) (1) (de) (1) (df) (1) (dg) (1) (dh) (1) (di) (1) (dj) (1) (dk) (1) (dl) (1) (dm) (1) (dn) (1) (do) (1) (dp) (1) (dq) (1) (dr) (1) (ds) (1) (dt) (1) (du) (1) (dv) (1) (dw) (1) (dx) (1) (dy) (1) (dz) (1) (ea) (1) (eb) (1) (ec) (1) (ed) (1) (ee) (1) (ef) (1) (eg) (1) (eh) (1) (ei) (1) (ej) (1) (ek) (1) (el) (1) (em) (1) (en) (1) (eo) (1) (ep) (1) (eq) (1) (er) (1) (es) (1) (et) (1) (eu) (1) (ev) (1) (ew) (1) (ex) (1) (ey) (1) (ez) (1) (fa) (1) (fb) (1) (fc) (1) (fd) (1) (fe) (1) (ff) (1) (fg) (1) (fh) (1) (fi) (1) (fj) (1) (fk) (1) (fl) (1) (fm) (1) (fn) (1) (fo) (1) (fp) (1) (fq) (1) (fr) (1) (fs) (1) (ft) (1) (fu) (1) (fv) (1) (fw) (1) (fx) (1) (fy) (1) (fz) (1) (ga) (1) (gb) (1) (gc) (1) (gd) (1) (ge) (1) (gf) (1) (gg) (1) (gh) (1) (gi) (1) (gj) (1) (gk) (1) (gl) (1) (gm) (1) (gn) (1) (go) (1) (gp) (1) (gq) (1) (gr) (1) (gs) (1) (gt) (1) (gu) (1) (gv) (1) (gw) (1) (gx) (1) (gy) (1) (gz) (1) (ha) (1) (hb) (1) (hc) (1) (hd) (1) (he) (1) (hf) (1) (hg) (1) (hh) (1) (hi) (1) (hj) (1) (hk) (1) (hl) (1) (hm) (1) (hn) (1) (ho) (1) (hp) (1) (hq) (1) (hr) (1) (hs) (1) (ht) (1) (hu) (1) (hv) (1) (hw) (1) (hx) (1) (hy) (1) (hz) (1) (ia) (1) (ib) (1) (ic) (1) (id) (1) (ie) (1) (if) (1) (ig) (1) (ih) (1) (ii) (1) (ij) (1) (ik) (1) (il) (1) (im) (1) (in) (1) (io) (1) (ip) (1) (iq) (1) (ir) (1) (is) (1) (it) (1) (iu) (1) (iv) (1) (iw) (1) (ix) (1) (iy) (1) (iz) (1) (ja) (1) (jb) (1) (jc) (1) (jd) (1) (je) (1) (jf) (1) (jg) (1) (jh) (1) (ji) (1) (jj) (1) (jk) (1) (jl) (1) (jm) (1) (jn) (1) (jo) (1) (jp) (1) (jq) (1) (jr) (1) (js) (1) (jt) (1) (ju) (1) (jv) (1) (jw) (1) (jx) (1) (jy) (1) (jz) (1) (ka) (1) (kb) (1) (kc) (1) (kd) (1) (ke) (1) (kf) (1) (kg) (1) (kh) (1) (ki) (1) (kj) (1) (kk) (1) (kl) (1) (km) (1) (kn) (1) (ko) (1) (kp) (1) (kq) (1) (kr) (1) (ks) (1) (kt) (1) (ku) (1) (kv) (1) (kw) (1) (kx) (1) (ky) (1) (kz) (1) (la) (1) (lb) (1) (lc) (1) (ld) (1) (le) (1) (lf) (1) (lg) (1) (lh) (1) (li) (1) (lj) (1) (lk) (1) (ll) (1) (lm) (1) (ln) (1) (lo) (1) (lp) (1) (lq) (1) (lr) (1) (ls) (1) (lt) (1) (lu) (1) (lv) (1) (lw) (1) (lx) (1) (ly) (1) (lz) (1) (ma) (1) (mb) (1) (mc) (1) (md) (1) (me) (1) (mf) (1) (mg) (1) (mh) (1) (mi) (1) (mj) (1) (mk) (1) (ml) (1) (mm) (1) (mn) (1) (mo) (1) (mp) (1) (mq) (1) (mr) (1) (ms) (1) (mt) (1) (mu) (1) (mv) (1) (mw) (1) (mx) (1) (my) (1) (mz) (1) (na) (1) (nb) (1) (nc) (1) (nd) (1) (ne) (1) (nf) (1) (ng) (1) (nh) (1) (ni) (1) (nj) (1) (nk) (1) (nl) (1) (nm) (1) (nn) (1) (no) (1) (np) (1) (nq) (1) (nr) (1) (ns) (1) (nt) (1) (nu) (1) (nv) (1) (nw) (1) (nx) (1) (ny) (1) (nz) (1) (oa) (1) (ob) (1) (oc) (1) (od) (1) (oe) (1) (of) (1) (og) (1) (oh) (1) (oi) (1) (oj) (1) (ok) (1) (ol) (1) (om) (1) (on) (1) (oo) (1) (op) (1) (oq) (1) (or) (1) (os) (1) (ot) (1) (ou) (1) (ov) (1) (ow) (1) (ox) (1) (oy) (1) (oz) (1) (pa) (1) (pb) (1) (pc) (1) (pd) (1) (pe) (1) (pf) (1) (pg) (1) (ph) (1) (pi) (1) (pj) (1) (pk) (1) (pl) (1) (pm) (1) (pn) (1) (po) (1) (pp) (1) (pq) (1) (pr) (1) (ps) (1) (pt) (1) (pu) (1) (pv) (1) (pw) (1) (px) (1) (py) (1) (pz) (1) (qa) (1) (qb) (1) (qc) (1) (qd) (1) (qe) (1) (qf) (1) (qg) (1) (qh) (1) (qi) (1) (qj) (1) (qk) (1) (ql) (1) (qm) (1) (qn) (1) (qo) (1) (qp) (1) (qq) (1) (qr) (1) (qs) (1) (qt) (1) (qu) (1) (qv) (1) (qw) (1) (qx) (1) (qy) (1) (qz) (1) (ra) (1) (rb) (1) (rc) (1) (rd) (1) (re) (1) (rf) (1) (rg) (1) (rh) (1) (ri) (1) (rj) (1) (rk) (1) (rl) (1) (rm) (1) (rn) (1) (ro) (1) (rp) (1) (rq) (1) (rr) (1) (rs) (1) (rt) (1) (ru) (1) (rv) (1) (rw) (1) (rx) (1) (ry) (1) (rz) (1) (sa) (1) (sb) (1) (sc) (1) (sd) (1) (se) (1) (sf) (1) (sg) (1) (sh) (1) (si) (1) (sj) (1) (sk) (1) (sl) (1) (sm) (1) (sn) (1) (so) (1) (sp) (1) (sq) (1) (sr) (1) (ss) (1) (st) (1) (su) (1) (sv) (1) (sw) (1) (sx) (1) (sy) (1) (sz) (1) (ta) (1) (tb) (1) (tc) (1) (td) (1) (te) (1) (tf) (1) (tg) (1) (th) (1) (ti) (1) (tj) (1) (tk) (1) (tl) (1) (tm) (1) (tn) (1) (to) (1) (tp) (1) (tq) (1) (tr) (1) (ts) (1) (tt) (1) (tu) (1) (tv) (1) (tw) (1) (tx) (1) (ty) (1) (tz) (1) (ua) (1) (ub) (1) (uc) (1) (ud) (1) (ue) (1) (uf) (1) (ug) (1) (uh) (1) (ui) (1) (uj) (1) (uk) (1) (ul) (1) (um) (1) (un) (1) (uo) (1) (up) (1) (uq) (1) (ur) (1) (us) (1) (ut) (1) (uu) (1) (uv) (1) (uw) (1) (ux) (1) (uy) (1) (uz) (1) (va) (1) (vb) (1) (vc) (1) (vd) (1) (ve) (1) (vf) (1) (vg) (1) (vh) (1) (vi) (1) (vj) (1) (vk) (1) (vl) (1) (vm) (1) (vn) (1) (vo) (1) (vp) (1) (vq) (1) (vr) (1) (vs) (1) (vt) (1) (vu) (1) (vv) (1) (vw) (1) (vx) (1) (vy) (1) (vz) (1) (wa) (1) (wb) (1) (wc) (1) (wd) (1) (we) (1) (wf) (1) (wg) (1) (wh) (1) (wi) (1) (wj) (1) (wk) (1) (wl) (1) (wm) (1) (wn) (1) (wo) (1) (wp) (1) (wq) (1) (wr) (1) (ws) (1) (wt) (1) (wu) (1) (wv) (1) (ww) (1) (wx) (1) (wy) (1) (wz) (1) (xa) (1) (xb) (1) (xc) (1) (xd) (1) (xe) (1) (xf) (1) (xg) (1) (xh) (1) (xi) (1) (xj) (1) (xk) (1) (xl) (1) (xm) (1) (xn) (1) (xo) (1) (xp) (1) (xq) (1) (xr) (1) (xs) (1) (xt) (1) (xu) (1) (xv) (1) (xw) (1) (xx) (1) (xy) (1) (xz) (1) (ya) (1) (yb) (1) (yc) (1) (yd) (1) (ye) (1) (yf) (1) (yg) (1) (yh) (1) (yi) (1) (yj) (1) (yk) (1) (yl) (1) (ym) (1) (yn) (1) (yo) (1) (yp) (1) (yq) (1) (yr) (1) (ys) (1) (yt) (1) (yu) (1) (yv) (1) (yw) (1) (yx) (1) (yy) (1) (yz) (1) (za) (1) (zb) (1) (zc) (1) (zd) (1) (ze) (1) (zf) (1) (zg) (1) (zh) (1) (zi) (1) (zj) (1) (zk) (1) (zl) (1) (zm) (1) (zn) (1) (zo) (1) (zp) (1) (zq) (1) (zr) (1) (zs) (1) (zt) (1) (zu) (1) (zv) (1) (zw) (1) (zx) (1) (zy) (1) (zz) (1)

CLASSIFIED DOCUMENT

This document contains classified information affecting the National Defense of the United States within the meaning of the Espionage Act, USC 50:31 and 32. Its transmission or the revelation of its contents in any manner to an unauthorized person is prohibited by law. Information so classified may be imparted only to persons in the military and naval services of the United States, appropriate civilian officers and employees of the Federal Government who have a legitimate interest therein, and to United States citizens of known loyalty and discretion who of necessity must be informed thereof.

NATIONAL ADVISORY COMMITTEE
FOR AERONAUTICS

WASHINGTON

September 5, 1951

Final
3-25-68

UNCLASSIFIED

8-14-68

UNCLASSIFIED

~~CONFIDENTIAL~~

NATIONAL ADVISORY COMMITTEE FOR AERONAUTICS

RESEARCH MEMORANDUM

A FLIGHT INVESTIGATION OF THE DAMPING IN ROLL AND ROLLING EFFECTIVENESS INCLUDING AEROELASTIC EFFECTS OF ROCKET-PROPELLED MISSILE MODELS HAVING CRUCIFORM, TRIANGULAR, INTERDIGITATED WINGS AND TAILS

By Russell N. Hopko

SUMMARY

The damping in roll and rolling effectiveness of two models of a missile having cruciform, triangular, interdigitated wings and tails have been determined through a Mach number range of 0.8 to 1.8 by utilizing rocket-propelled test vehicles. Results indicate that the damping in roll was relatively constant over the Mach number range investigated. The rolling effectiveness was essentially constant at low supersonic speeds and increased with increasing Mach numbers in excess of 1.4 over the Mach number range investigated. Aeroelastic effects increase the rolling-effectiveness parameter $\frac{pb}{2V} \delta$ and decrease both the rolling-moment coefficient $C_{L\delta}$ and the damping-in-roll coefficient $C_{L\dot{\alpha}}$.

INTRODUCTION

The Pilotless Aircraft Research Division of the Langley Aeronautical Laboratory is investigating some of the aerodynamic characteristics of a missile having cruciform, triangular, interdigitated wings and tails by utilizing rocket-propelled test vehicles. One phase of the program, the measurement of the variation of zero-lift drag with Mach number for several missile configurations, has been completed and the results reported (reference 1). Another phase of the program, the investigation of the longitudinal stability and control characteristics is being made. Results of the first flight test in this phase are reported in reference 2. An investigation of the damping in roll and rolling effectiveness has been completed and the results are reported herein.

CLASSIFICATION CHANGED

UNCLASSIFIED

CLASSIFICATION CHANGED

UNCLASSIFIED

By Russell N. Hopko
10/14/67
New York, N.Y.
1-12-68

1-26-68

3-7-67

NASA CRU 143

8-14-68

~~CONFIDENTIAL~~

UNCLASSIFIED

The flight tests were conducted at the Pilotless Aircraft Research Station, Wallops Island, Va.

SYMBOLS

C_{lp}	damping-in-roll coefficient $\left(\Delta C_l / \Delta \frac{pb}{2V}\right)$
$C_l =$	$\frac{\text{Rolling moment}}{qSb}$
T	torque, foot-pounds
p	angular velocity
$\frac{pb}{2V}$	wing-tip helix angle, radians
V	velocity, feet per second
$C_{l\delta}$	rolling-moment coefficient due to wing deflection $(\partial C_l / \partial \delta)$
C_D	drag coefficient based on cross-sectional area of fuselage (0.442 sq ft)
q	dynamic pressure, pounds per square foot
S	exposed area of two wings, square feet
b	wing span, feet
M	Mach number
P	ambient static pressure, pounds per square inch
E	modulus of elasticity, pounds per square inch
δ	wing deflection angle, degrees
R	Reynolds number, based on wing mean aerodynamic chord of gross area

Subscripts:

w	wing
t	tail

θ twist
 δ wing deflection

MODELS AND TESTS

Model 1

The general arrangement of model 1 is shown in figures 1 and 2 and a photograph of model 1 is shown in figure 3. Some physical characteristics of model 1 are shown in tables I and II.

Model 1 has a cylindrical body with an ogival nose of fineness ratio 6.25, cruciform triangular wings of aspect ratio 2.3, and cruciform triangular tails of aspect ratio 4 with wings and tails interdigitated.

The fuselage was constructed of 0.064-inch 75S-T6 aluminum alloy with ring stiffeners. The wing and tail fuselage sections, the wings, and the tails were forged and machined from aluminum alloy. Each of the four wings was set at 3° deflection to produce roll.

The model was propelled to a Mach number of about 0.5 by a special booster rocket motor. Following the boost period, an ABL Deacon rocket motor propelled the model to a Mach number of 1.92. The ABL Deacon rocket motor was equipped with a nozzle assembly having four small canted nozzles which produced both thrust and a rolling moment during the powered flight. A photograph of the model and booster on the launcher is shown in figure 4.

A standard NACA telemeter was installed in the nose section. Quantities measured included total pressure, rolling velocity, longitudinal acceleration, and rocket chamber pressure. During flight the model was tracked with CW Doppler radar to determine velocity and SCR 584 radar to determine the flight path. Atmospheric data were determined by radio-sonde measurements. The damping-in-roll derivative was calculated from the increment in rolling velocity at a given Mach number by using equations of equilibrium in roll during power-on and power-off flight. The rolling moment due to the torque nozzle was calculated from the measured chamber pressure with the use of a calibration obtained in static firings. A complete description of the canted-nozzle technique may be found in reference 3.

The rolling-effectiveness parameter $\frac{pb}{2V/\delta}$ was determined during coasting flight.

Model 2

The general arrangement of model 2 and test vehicle is shown in figure 5. A photograph of the model is shown in figure 6 and a photograph of the model and test vehicle combination is shown in figure 7.

The fuselage of model 2 was machined from 24S-T aluminum and the wings and tails were of S.A.E. 4130 steel. The four wings were set at 0° deflection angle.

The model was sting mounted to the nose of the test vehicle. Relative displacement in roll between the model and the test vehicle was measured by a torsion-spring balance in the nose of the test vehicle. Stabilizing fins set at an angle of deflection forced the model and test vehicle to roll. Histories of model rolling moment, model rolling velocity, and flight-path velocity were obtained by using standard NACA procedures. These data were used in conjunction with atmospheric data obtained with radiosonde to determine C_{lp} . A complete description of this technique may be found in reference 4.

The variation of Reynolds number with Mach number for the various investigations is shown in figure 8.

ACCURACY

The errors in the results are estimated to be within the following limits:

M	$\frac{pb}{2V/\delta}$	C_{lp}		$C_{l\delta}$
	Model 1	Model 1	Model 2	Model 1
0.9	±0.0007	±0.05	±0.08	±0.001
1.2	±0.0005	±0.05	±0.04	±0.001
1.5	±0.0003	±0.05	±0.03	±0.001

These errors are systematic in nature; the variations and trends shown in the results for each model are subject to much smaller errors.

The error in wing deflection δ is estimated to be within ±0.01°.

RESULTS AND DISCUSSION

The measured variation of the wing-tip helix angle $pb/2V$ with Mach number obtained with model 1 is shown in figure 9 for power-on and power-off flight. Also shown is the steady-state ($\frac{dp}{dt} = 0$) variation of $pb/2V$ with Mach number obtained by correcting the measured values of $pb/2V$ for the effect of angular acceleration about the roll axis. Also shown in figure 9 is the variation of rolling-moment coefficient due to the torque nozzle with Mach number.

The variation of C_l (the rolling-moment coefficient of the test model) and $pb/2V$ (the wing-tip helix angle of the test model) with Mach number obtained with model 2 is shown in figure 10.

Damping in Roll

The variation of the damping-in-roll coefficient C_{l_p} with Mach number obtained with model 1 by the method of reference 3 is shown in figure 11. Also shown in figure 11 is the variation of C_{l_p} with Mach number, obtained with model 2, calculated from the quantities of figure 10. The results shown in figure 11 indicate that the damping in roll was relatively constant over the Mach number range investigated. The measured values of damping are less than theoretical values obtained by calculating (and adding) the damping in roll of the individual cruciform wing and tail assemblies according to references 5 and 6. Shown also in figure 11 are values of C_{l_p} obtained by wind-tunnel tests of a similar configuration (reference 7). Excellent agreement is shown between model 2 and the 0.135-scale model wind-tunnel-test results. Flight-test results obtained with model 1 show less damping in roll than the flight-test results obtained with model 2.

The differences noted in figure 11 between the experimental results of model 1 and model 2 are believed to be due primarily to aeroelastic effects for the following reasons:

From simple considerations it can be seen that, at a given Mach number, the loss in damping in roll due to aeroelastic effects varies linearly with the ambient static pressure P and with the reciprocal of the modulus of elasticity $1/E$. The variation of C_{l_p} with P/E is shown in figure 12 for $M = 1.6$ where the values of C_{l_p} are those determined by tests and the values of P are the ambient static pressures under test conditions and E is the modulus of elasticity of the

material used for the wing and tail surfaces of the models. Also shown in figure 12 is an estimated rigid value, obtained as described in the appendix, for model 1 at a Mach number of 1.6. The curve joining these two points is the estimated variation of C_{l_p} with P/E for model 1.

The interpolated (essentially rigid) wind-tunnel value (reference 7) agrees well. Test results of model 2 are slightly higher, probably because of differences in wing and tail root restraint and wing-gap effect. Model 2 and the wind-tunnel model had steel wings and tail surfaces with full-chord root attachments; the wing and tail surfaces of model 1 were of aluminum alloy, the tail root attachment was only partial chord (fig. 1), and the wing root attachment consisted of a trunnion and a wing adjustment tab. Root restraint has an important effect on the wing and tail deflection patterns. Results from load tests of a wing similar to model 1 with modification to give a full-chord root attachment show approximately 40 percent less wing twist than the results obtained from load tests of a wing identical to that of model 1. No similar tests were made of the tail. The value of C_{l_p} determined by the curve at $\frac{P}{E} = 0$ is lower than that obtained by summing the theoretical values of damping in roll of the individual cruciform wings and tails. The difference is due to the effects of wing-body-tail interference, wing-body-gap, root restraint, wing thickness, and viscous effects.

Rolling Effectiveness

Figure 13 shows the steady-state power-off values of $\frac{pb}{2V/\delta}$ obtained during coasting flight with model 1. The variation of C_{l_δ} with Mach number, obtained with model 1, calculated by using steady-state power-off values of $\frac{pb}{2V/\delta}$ from figure 13 and values of C_{l_p} from figure 11 is also shown in figure 13. These results indicate that the rolling effectiveness was constant at low supersonic speeds and increased with increasing Mach numbers in excess of 1.4 over the Mach number range investigated. Shown also are values of $\frac{pb}{2V/\delta}$ calculated by using supersonic wind-tunnel values of C_{l_p} and C_{l_δ} from references 7 and 8, respectively. Values of $\frac{pb}{2V/\delta}$ calculated from wind-tunnel tests are lower than those obtained in flight with model 1. Calculations by the method outlined in the appendix indicate that most of the difference in the values of $\frac{pb}{2V/\delta}$ obtained in free flight and wind-tunnel tests is due to a loss in effective tail damping due to twist in the tail surfaces under load. Also shown in figure 13 are wind-tunnel values of C_{l_δ} from references 8 and 9. The estimated rigid values of C_{l_δ} calculated by the method outlined in the appendix for $M = 1.6$ agree well with essentially rigid, supersonic wind-tunnel values.

Drag Measurements

The variation of the drag coefficient C_D with Mach number obtained during power-off rolling flight with model 1 is shown in figure 14. Also shown are no-roll results from reference 1. The increment in drag which is due to the combined effects of wing deflection and rolling velocity is relatively large at the lower supersonic speeds and becomes smaller with increasing Mach number.

CONCLUSIONS

The following conclusions are indicated from the tests reported herein of two models of a missile having cruciform, triangular, interdigitated wings and tails:

1. Damping in roll was relatively constant over the Mach number range investigated.

2. Rolling effectiveness was constant at the low supersonic speeds and increased with increasing Mach numbers in excess of 1.4 over the Mach number range investigated.

3. Aeroelastic effects increase the rolling-effectiveness parameter $\frac{pb}{2V} \delta$ and decrease both the rolling-moment coefficient $C_{l\delta}$ and the damping-in-roll coefficient C_{l_p} .

Langley Aeronautical Laboratory
National Advisory Committee for Aeronautics
Langley Field, Va.

APPENDIX

EFFECT OF AEROELASTICITY AT $M = 1.6$

Static load tests of simulated supersonic air loads at a Mach number of 1.6 and a dynamic pressure of 3480 pounds per square foot during powered flight and 2670 pounds per square foot during power-off flight were made of wing and tail surfaces identical to those of model 1 to estimate the aeroelastic effects of the wing and tail surfaces on the damping in roll and rolling effectiveness for this missile configuration. The estimation was made by the following method:

For model 1, the damping-in-roll coefficient C_{l_p} and the rolling-effectiveness parameters C_{l_δ} and $\frac{pb}{2V}/\delta$ were determined from measurements of model rate of roll during power-on and power-off flight. The problem was, therefore, to determine the rate of roll which a rigid configuration would have had at the same conditions. The determination of the rate of roll for the rigid configuration in powered flight consisted of evaluating the following equation of equilibrium in roll:

$$T + \delta L_\delta = p \left[L_{p_w} + L_{p_t} + (L_{\theta_p})_w + (L_{\theta_p})_t \right] + \delta (L_{\theta_\delta})_w + L_0 + L_i$$

where T is the rolling moment produced by the torque nozzle, δL_δ is the rolling moment produced by differential deflection of four wings, L_p is the dimensional damping-in-roll derivative, $(L_{\theta_p})_w$ is the rate of change of rolling moment produced by aeroelastic deflections caused by the loading due to rate of roll with rate of roll, $(L_{\theta_\delta})_w$ is the rate of change of rolling moment produced by aeroelastic deflections caused by loadings due to the differential deflection of four wings with deflection, L_0 is the moment due to out of trim, and L_i is the moment due to interference.

In the equation of equilibrium T was the measured torque, L_δ was obtained from reference 5, L_{p_w} was obtained from reference 10, and L_{p_t} was obtained from references 6 and 11. The factor $(L_{\theta_\delta})_w$ was obtained by the following aeromechanical iteration process: The initial rigid-surface load distribution, obtained from reference 5, was placed on the wing by means of distributed concentrated loads. Figure 15 is a photograph of a typical test setup. The local streamwise surface slope at

each of the loading points produced by the initial loading was obtained by interpolations between dial-gage locations. The incremental load due to this deflection was obtained by taking a proportion of the initial load at the point in the ratio of the change in slope to the initial slope. The incremental loading was applied and the deflections measured. At this point it was calculated that the third incremental loading would produce deflections within the accuracy of the technique. The factors $(L_{\theta_p})_w$ and $(L_{\theta_p})_t$ were obtained similarly with the use of initial rigid-surface load distributions from references 10, 11, and 6.

The foregoing quantities were inserted into the equation of equilibrium to obtain a rolling velocity p_f for the flexible condition. The equation was also solved by assuming $L_{\theta_p} = L_{\theta_\delta} = 0$ to obtain a rolling velocity p_r for the rigid condition. A factor equal to $\frac{p_f - p_r}{p_r}$ was applied to the measured power-on rate of roll to obtain the rate of roll which would have been obtained with a rigid structure. It will be noted that the effect of neglecting the interference rolling moments in the equation of equilibrium is minimized by applying the factor $\frac{p_f - p_r}{p_r}$ to the rates of roll measured in flight.

The foregoing procedure was also applied to the power-off condition where $T = 0$.

The value of C_{l_p} for the rigid configuration was determined with the use of the increment in $\frac{pb}{2V}\delta$ calculated for the rigid configuration and the rolling-moment coefficient due to the torque nozzle.

The rolling-moment coefficient C_{l_δ} of the rigid configuration was then determined by using the rigid values of C_{l_p} and power-off $\frac{pb}{2V}\delta$. The effects of aeroelasticity due to wing and tail deformations are given in the following table:

	Measured in flight test	Estimated rigid values	Percent change from rigid value due to tail deformation	Percent change from rigid value due to wing deformation
$\frac{pb}{2V}$ (power-on)	0.0840	0.0605	31	8
$\frac{pb}{2V}$ (power-off)	.0185	.0141	31	0
C_{l_p}	-.420	-.640	-28	-6
C_{l_δ}	.0078	.0090	-7	-6

Values of C_{l_p} , $\frac{pb}{2V}/\delta$, and C_{l_δ} determined for the rigid configuration are shown in figures 12 and 13, respectively. It is interesting to note that for model 1, most of the loss in damping is due to the deformation of the tail surfaces.

It is seen that the rolling-effectiveness parameter $\frac{pb}{2V}/\delta$ is increased because of aeroelastic effects for this missile configuration and that the rolling-moment coefficient C_{l_δ} and the damping-in-roll coefficient C_{l_p} are decreased because of aeroelastic effects.

REFERENCES

1. Hall, James R., and Sandahl, Carl A.: Effect of Nose Shape and Wing Thickness Ratio on the Drag at Zero Lift of a Missile Having Triangular Wings and Tails. NACA RM L50C16a, 1950.
2. Sandahl, Carl A., and Hall, James R.: Free-Flight Investigation of the Longitudinal Stability and Control of a Rocket-Propelled Missile Model Having Cruciform, Triangular, Interdigitated Wings and Tails. NACA RM L51B15, 1951.
3. Edmondson, James L., and Sanders, E. Claude, Jr.: A Free-Flight Technique for Measuring Damping in Roll by Use of Rocket-Powered Models and Some Initial Results for Rectangular Wings. NACA RM L9101, 1949.
4. Bland, William M., Jr., and Sandahl, Carl A.: A Technique Utilizing Rocket-Propelled Test Vehicles for the Measurement of the Damping in Roll of Sting-Mounted Models and Some Initial Results for Delta and Unswept Tapered Wings. NACA RM L50D24, 1950.
5. Adams, Gaynor J.: Theoretical Damping in Roll and Rolling Effectiveness of Slender Cruciform Wings. NACA TN 2270, 1951.
6. Brown, Clinton E., and Adams, Mac C.: Damping in Pitch and Roll of Triangular Wings at Supersonic Speeds. NACA Rep. 892, 1948. (Formerly NACA TN 1566.)
7. Delameter, H. D., and Beal, R. R.: Analysis of Dynamic-Roll Characteristics from Supersonic Wind-Tunnel Tests of a 13.5-Percent-Scale Model of the Sparrow 13-D. Rep. No. SM-13628, Douglas Aircraft Co., Inc., Dec. 15, 1949.
8. Sager, B. F., Kutschinski, C. R., and Goldbaum, G. C.: Sparrow 13-D. Analysis of Force and Moment Characteristics from Supersonic Wind-Tunnel Tests of a 13.5-Percent-Scale Model. Rep. No. SM-13631, Douglas Aircraft Co., Inc., March 17, 1950.
9. Magnus, R. J., Beal, R. R., and Kutschinski, C. R.: Sparrow 13-D. Analysis of Force and Moment Characteristics from Subsonic Wind-Tunnel Tests of a 50-Percent-Scale Model. Rep. No. SM-13632, Douglas Aircraft Co., Inc., March 15, 1950.
10. Lomax, Harvard, and Heaslet, Max. A.: Damping-in-Roll Calculations for Slender Swept-Back Wings and Slender Wing-Body Combinations. NACA TN 1950, 1949.

11. Tucker, Warren A., and Piland, Robert O.: Estimation of the Damping in Roll of Supersonic-Leading-Edge Wing-Body Combinations. NACA TN 2151, 1950.

TABLE I
GENERAL PHYSICAL PROPERTIES OF MODELS TESTED

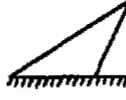
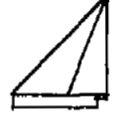
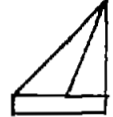
Model	Scale	Test	Tail and wing positions	Material of wing and tail	Wing thickness (t/c)	Tail thickness (t/c)	Wing root restraint	Tail root restraint
1	1.125	Free flight	Inter-digitated	14S-T4 aluminum	0.04	0.03		
2	.152	Free flight	Inter-digitated	S.A.E. 4130 steel	.04	.04		
3 (reference 7)	.135	Wind tunnel	In-line	Steel	.029	.030		



TABLE II

PHYSICAL CHARACTERISTICS OF MODEL 1

Over-all length, in.	143.28
Maximum diameter of constant section, in.	9.00
Weight (loaded), lbs	364.5
Weight (motor expended), lbs	264
Center-of-gravity (loaded) fuselage station, in.	74.12
Center-of-gravity (motor expended) fuselage station, in.	67.75
Exposed area of each wing, sq ft	1.6
Exposed area of each tail, sq ft	0.637
Wing thickness ratio, t/c	0.04
Tail thickness ratio, t/c	0.03
Wing deflection, deg	±3



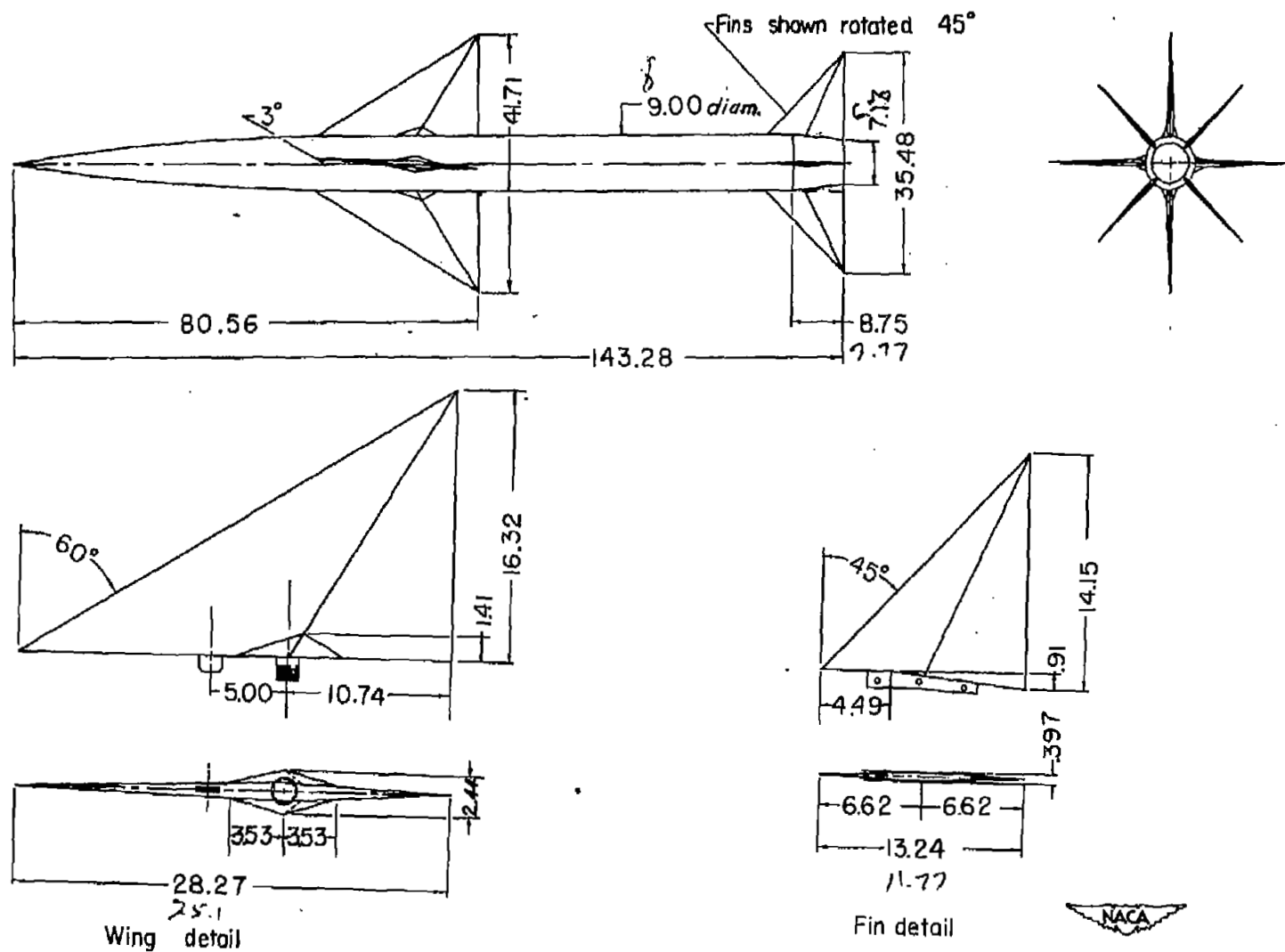


Figure 1.- General arrangement of model 1. All dimensions are in inches.



Figure 3.- Model 1.

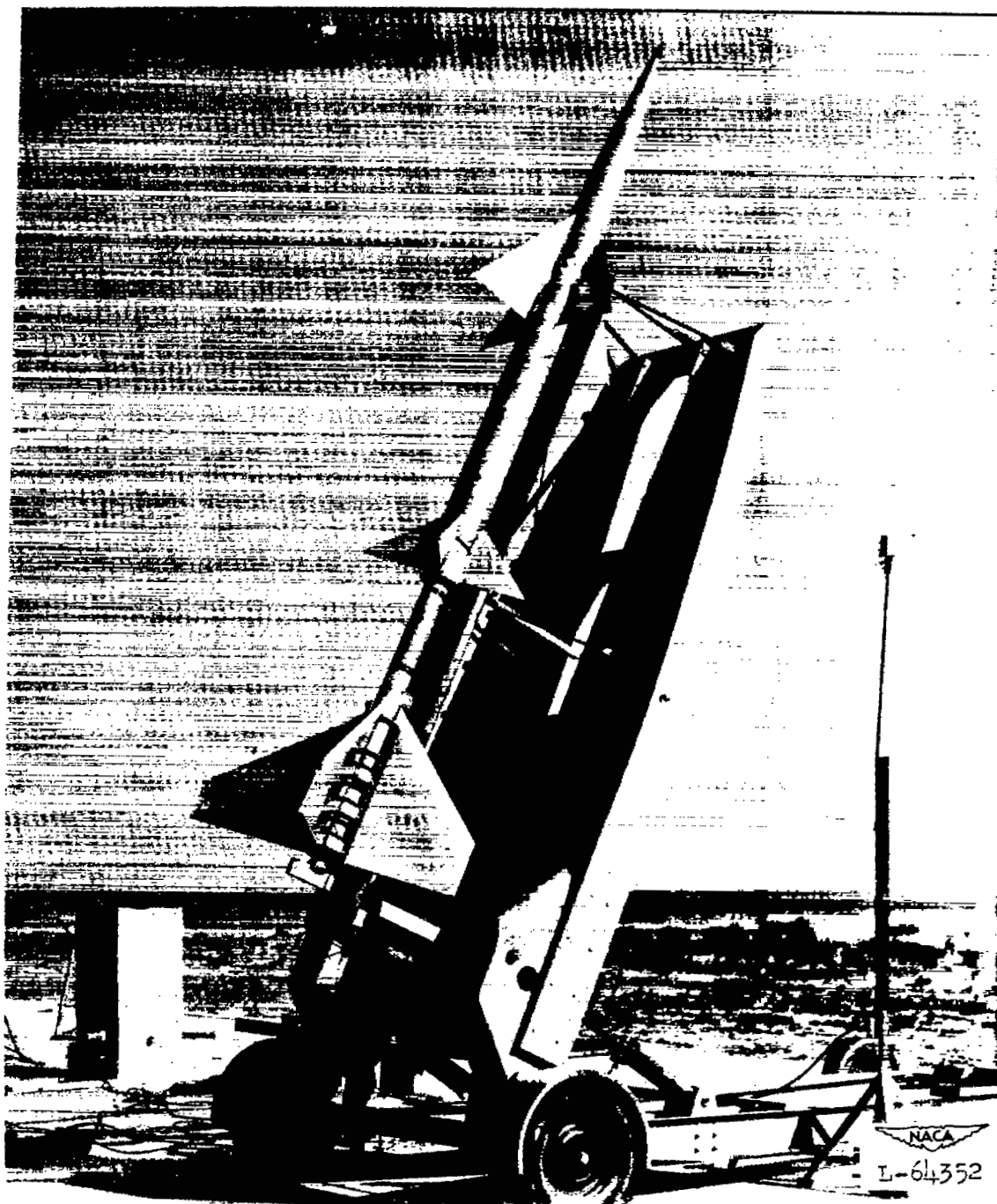


Figure 4.- Model 1 and booster on launcher.

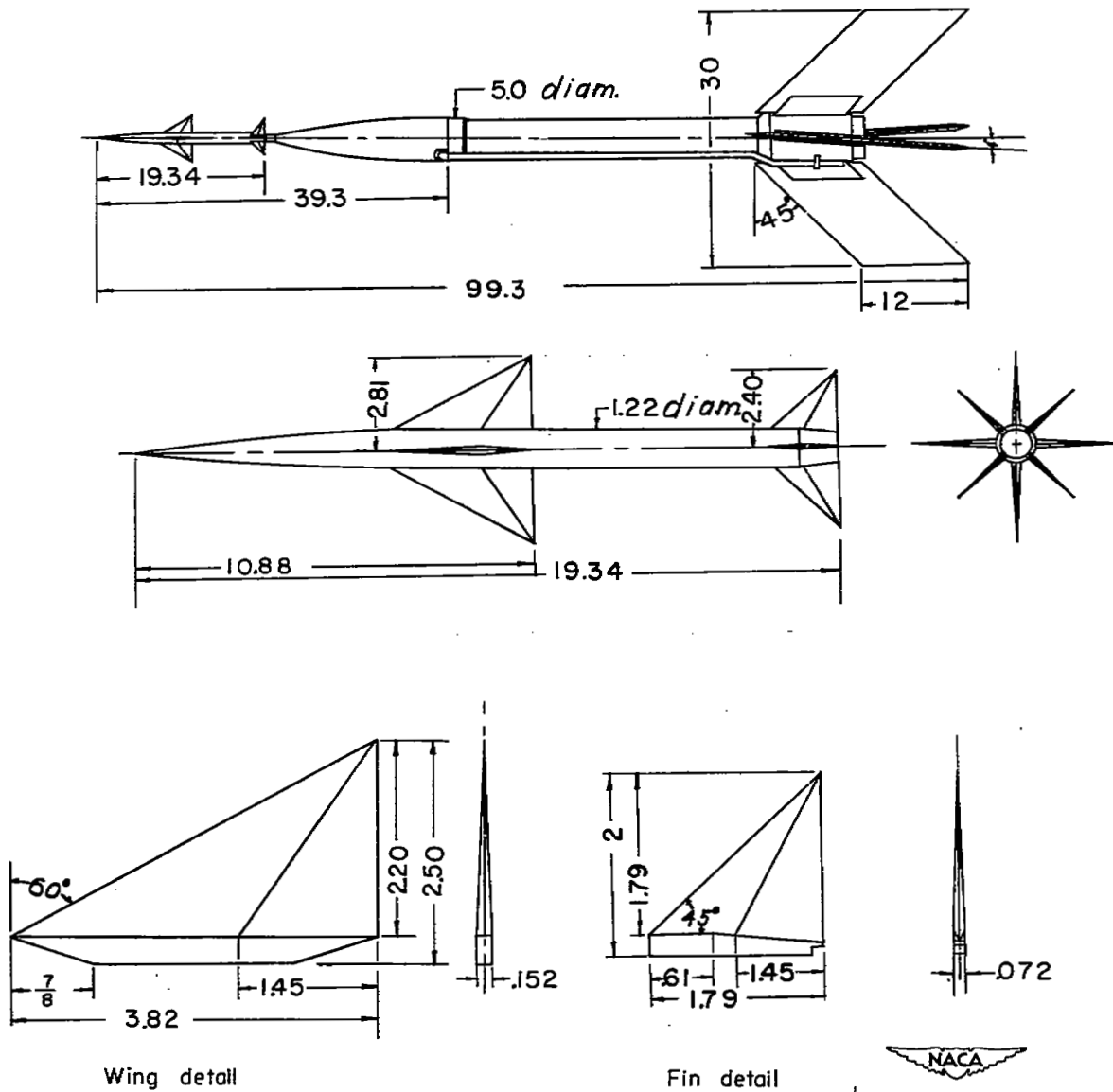


Figure 5.- General arrangement of model 2 and test vehicle. All dimensions are in inches.

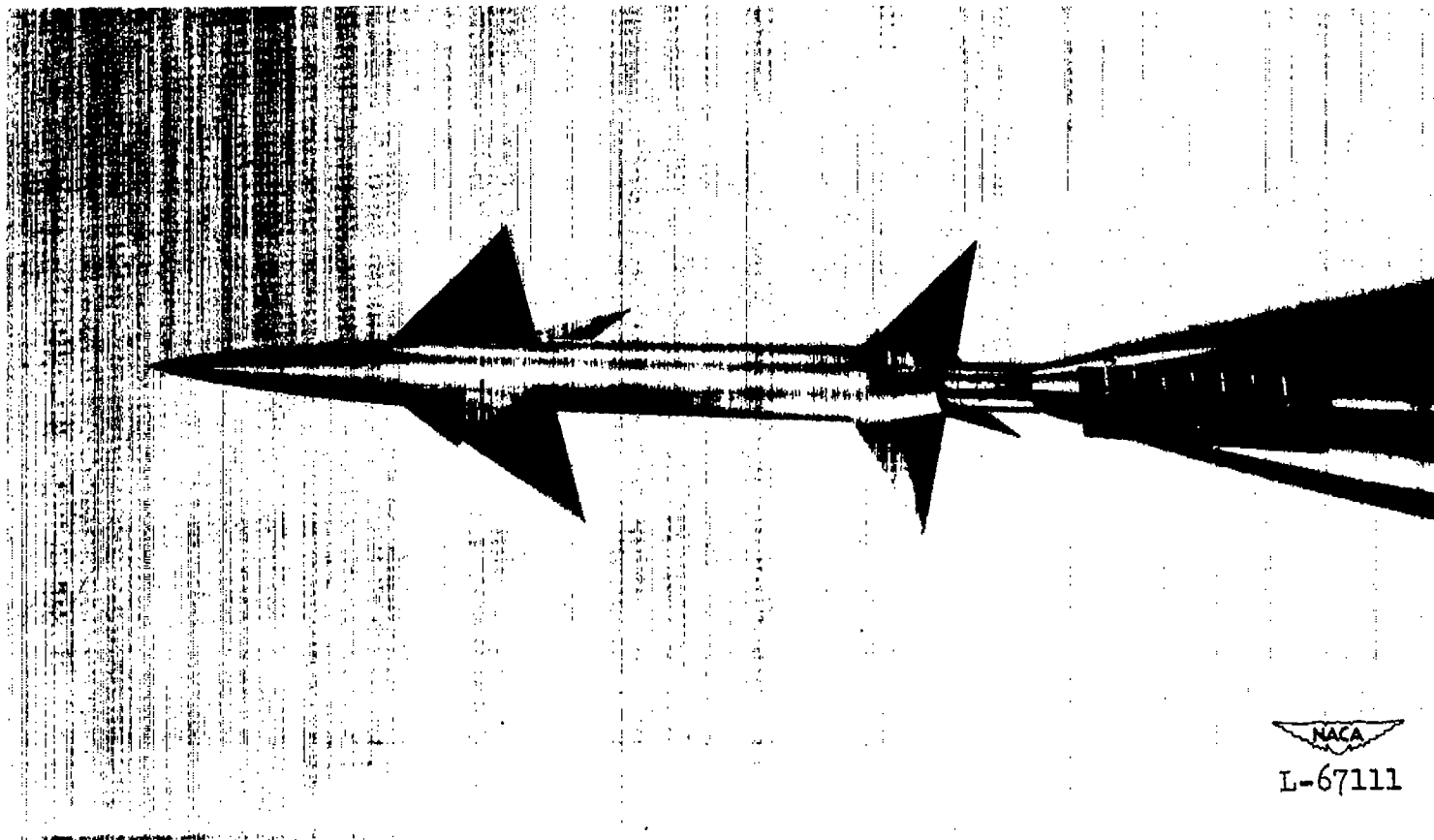


Figure 6.- Model 2.

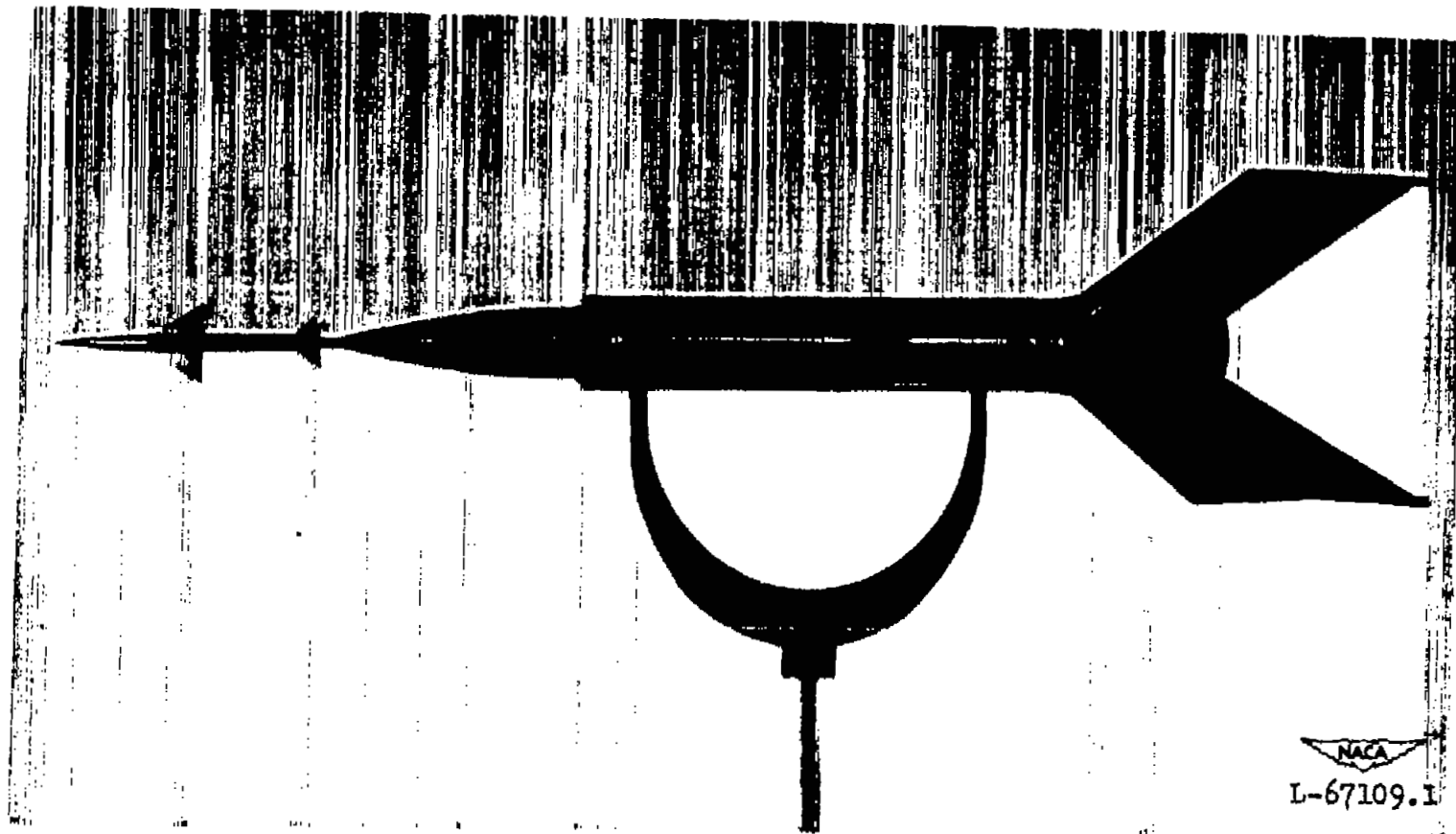


Figure 7.- Model 2 and test vehicle.

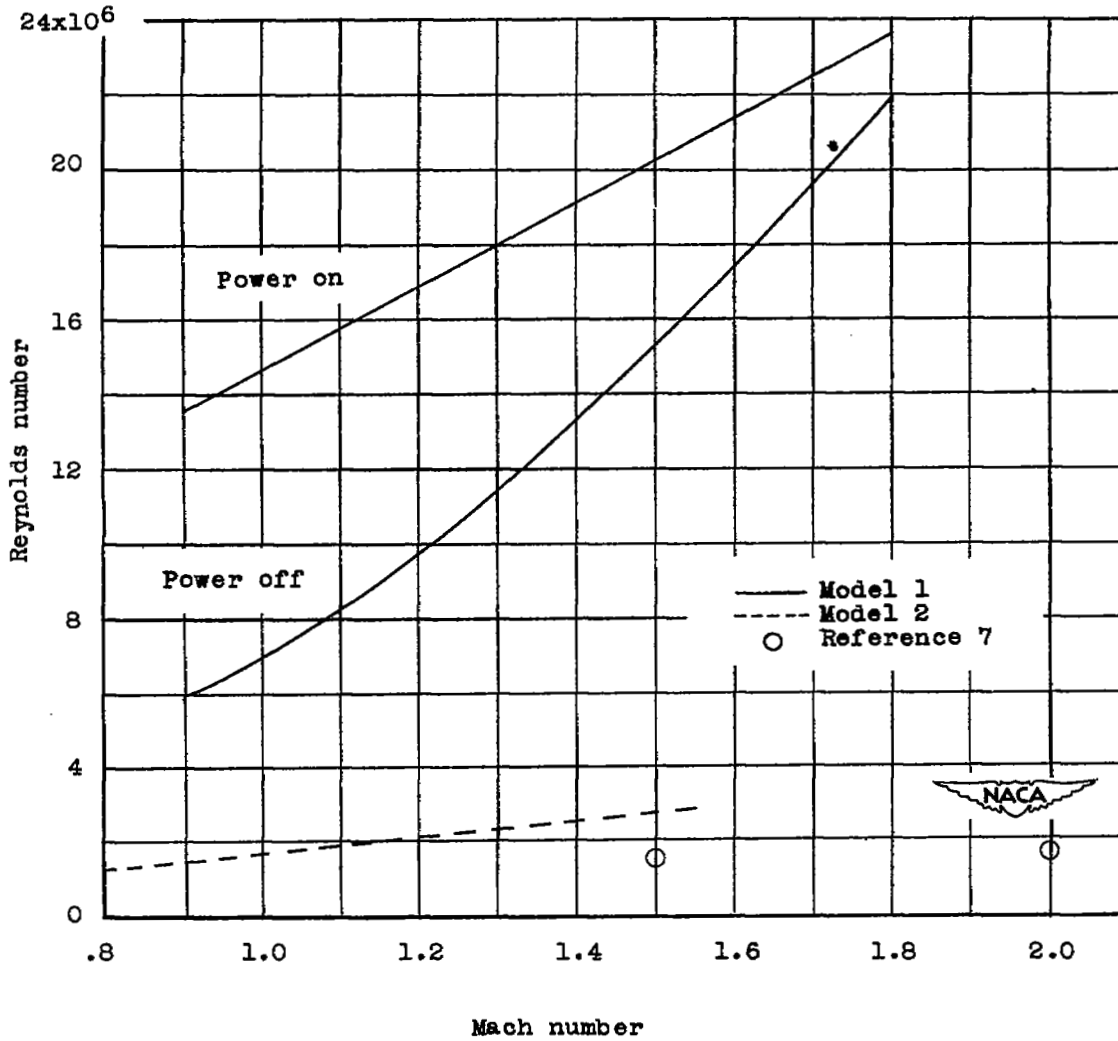


Figure 8.- Variation of Reynolds number, based on wing mean aerodynamic chord of gross wing area, with Mach number.

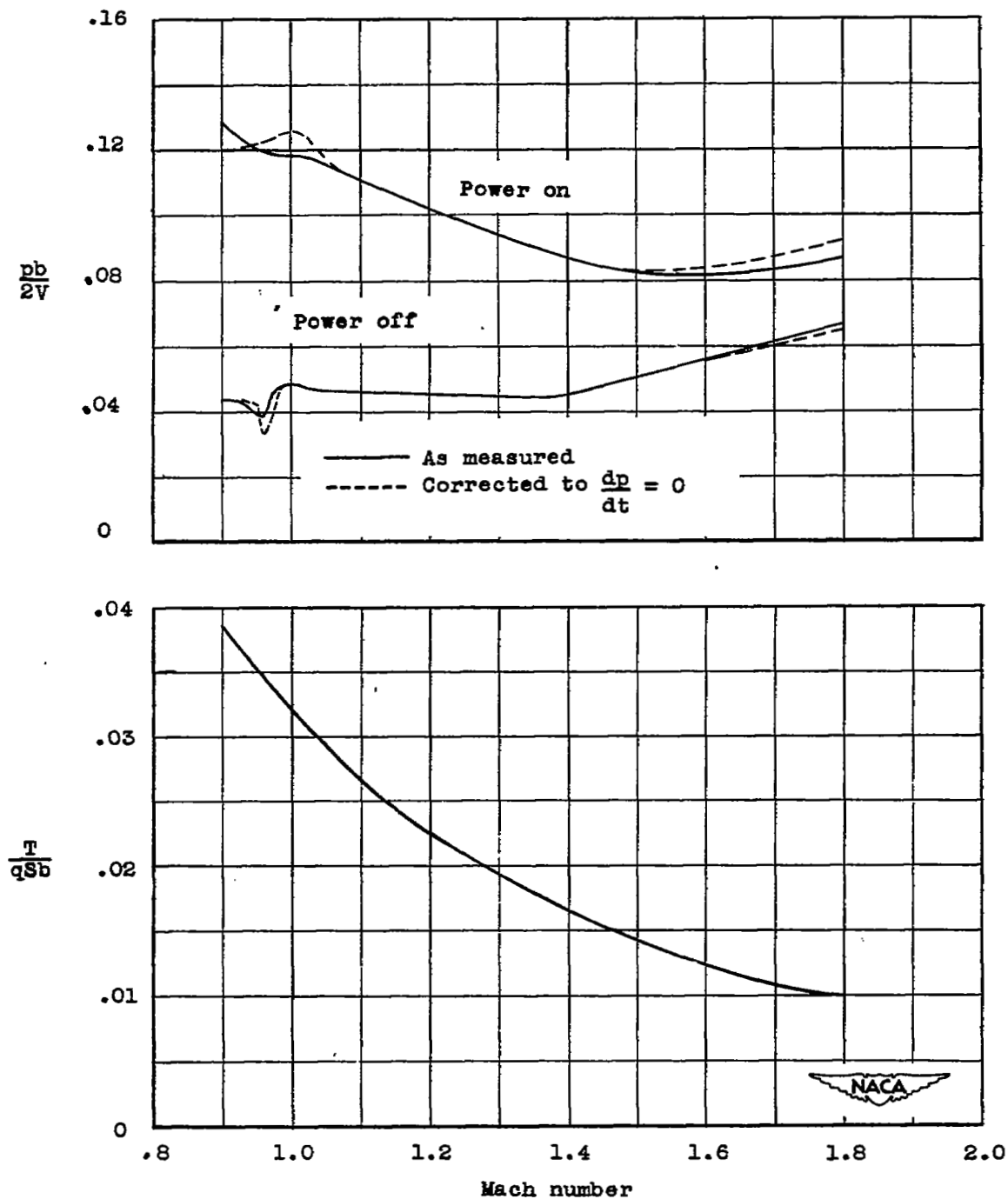


Figure 9.- Variation with Mach number of wing-tip helix angle and rolling-moment coefficient due to the torque nozzle for model 1.

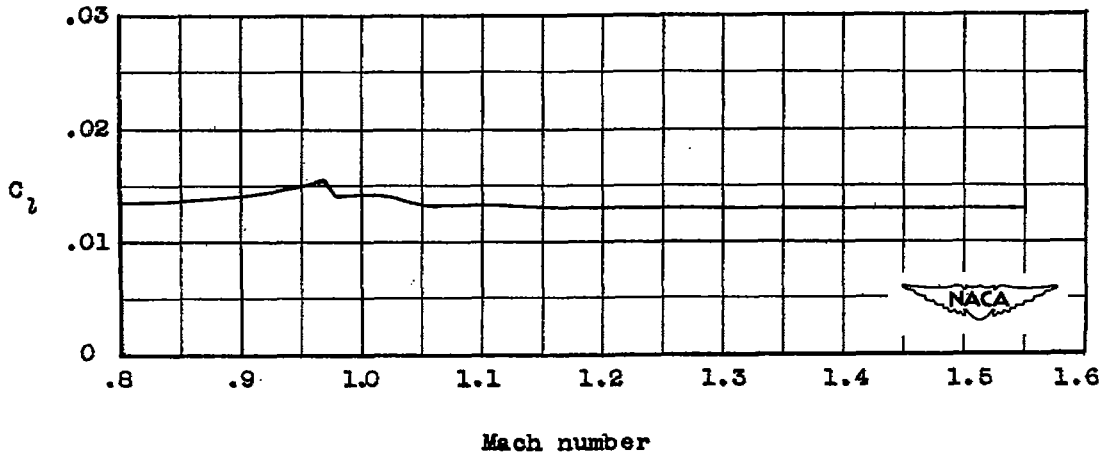
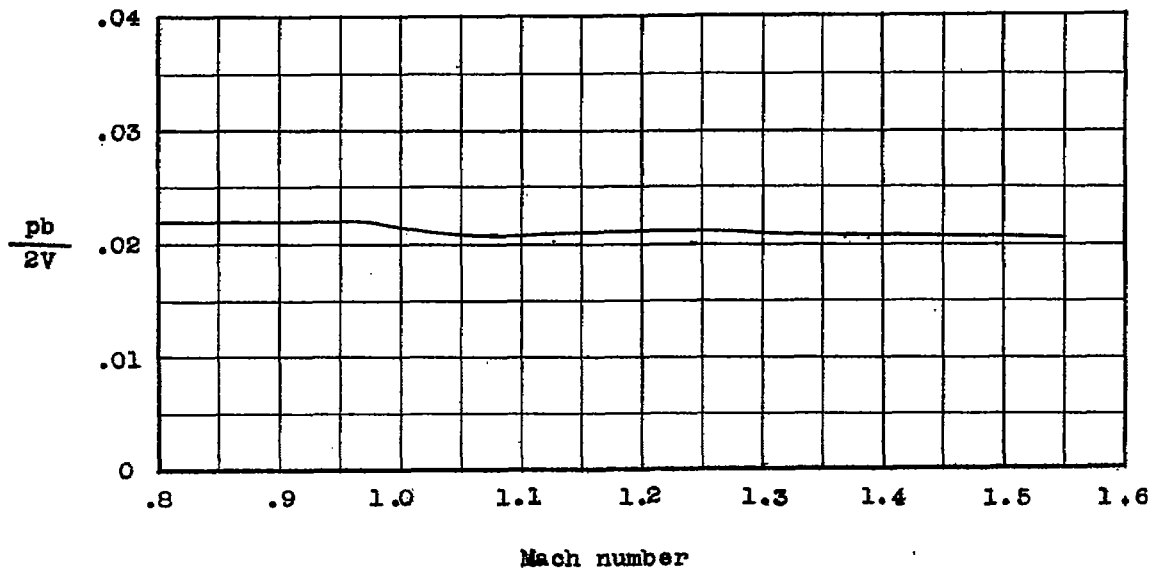


Figure 10.- Variation of wing-tip helix angle and rolling-moment coefficient with Mach number for model 2.

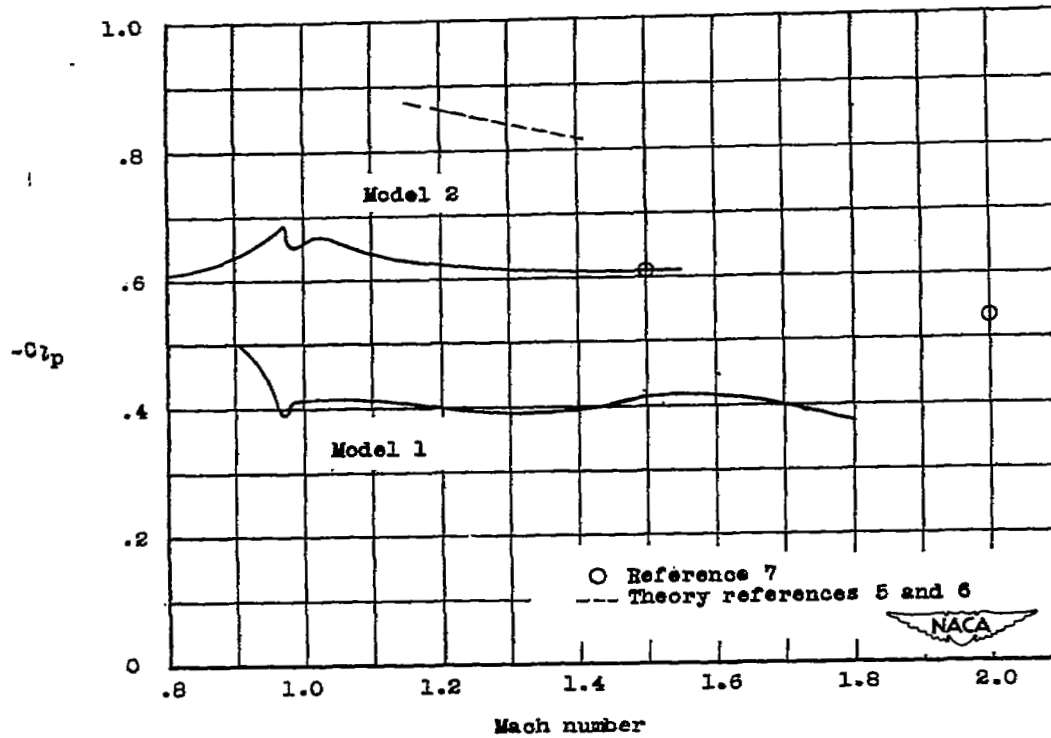


Figure 11.- Variation of C_{l_p} with Mach number.

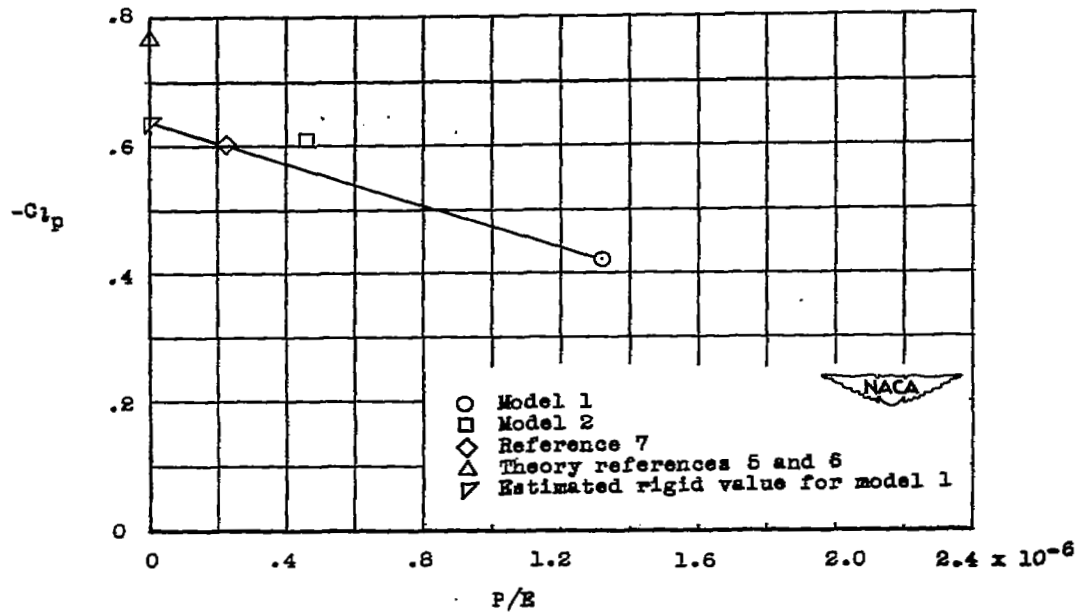


Figure 12.- Variation of C_{l_p} with P/E . $M = 1.6$.

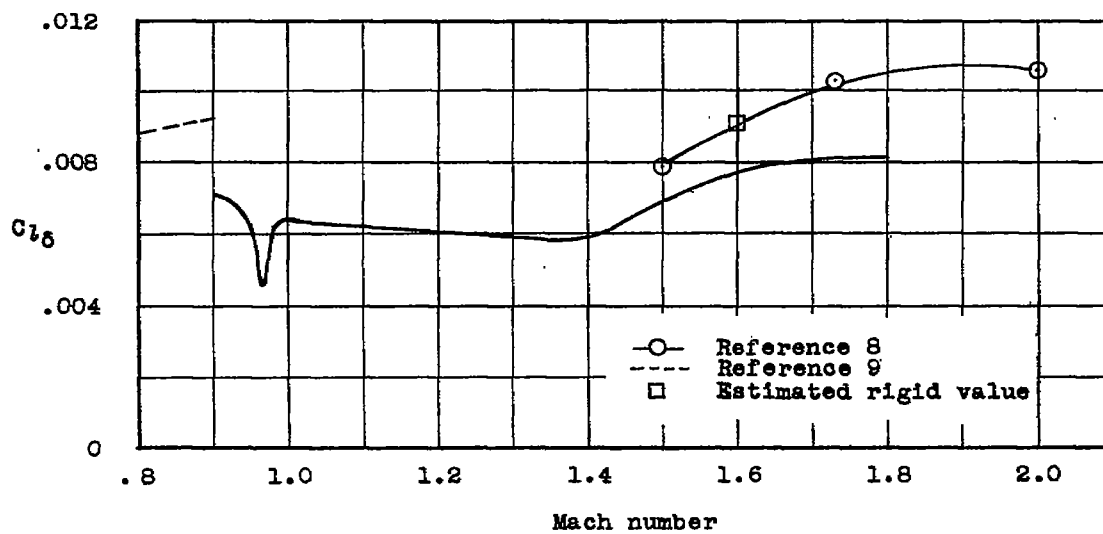
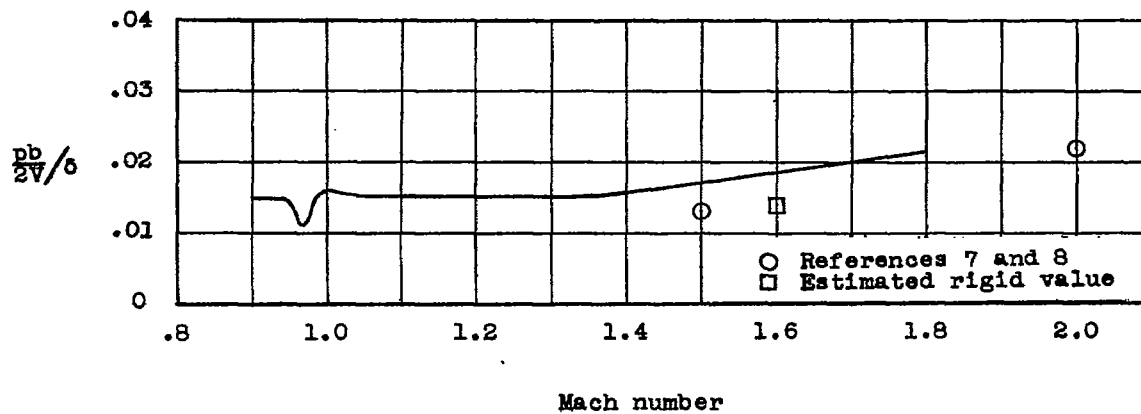


Figure 13.- Variation of rolling effectiveness with Mach number for model 1.

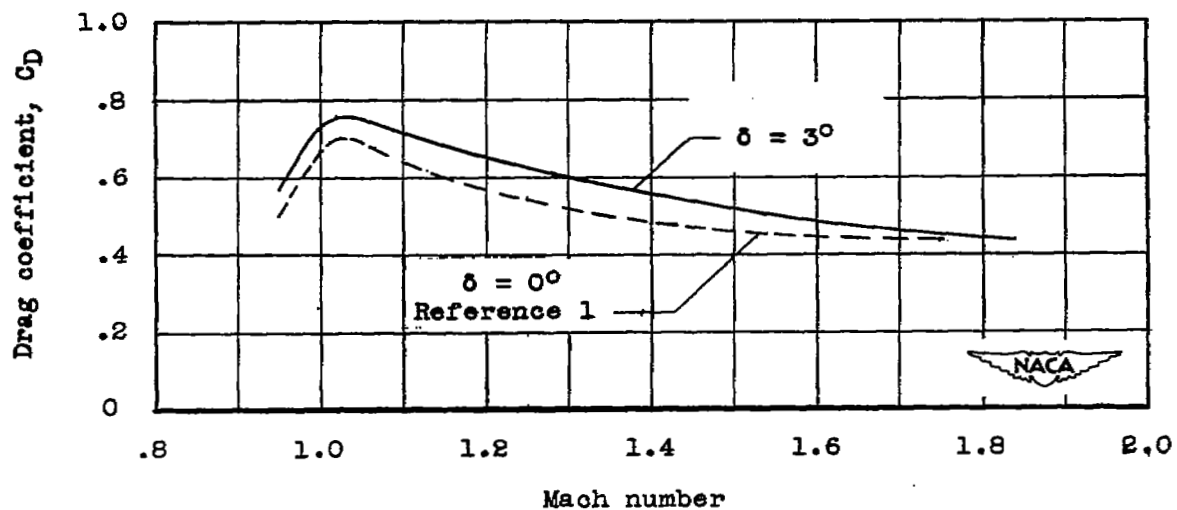


Figure 14.- Variation of drag coefficient with Mach number for model 1.

UNCLASSIFIED

~~CONFIDENTIAL~~

NACA RM L51D16

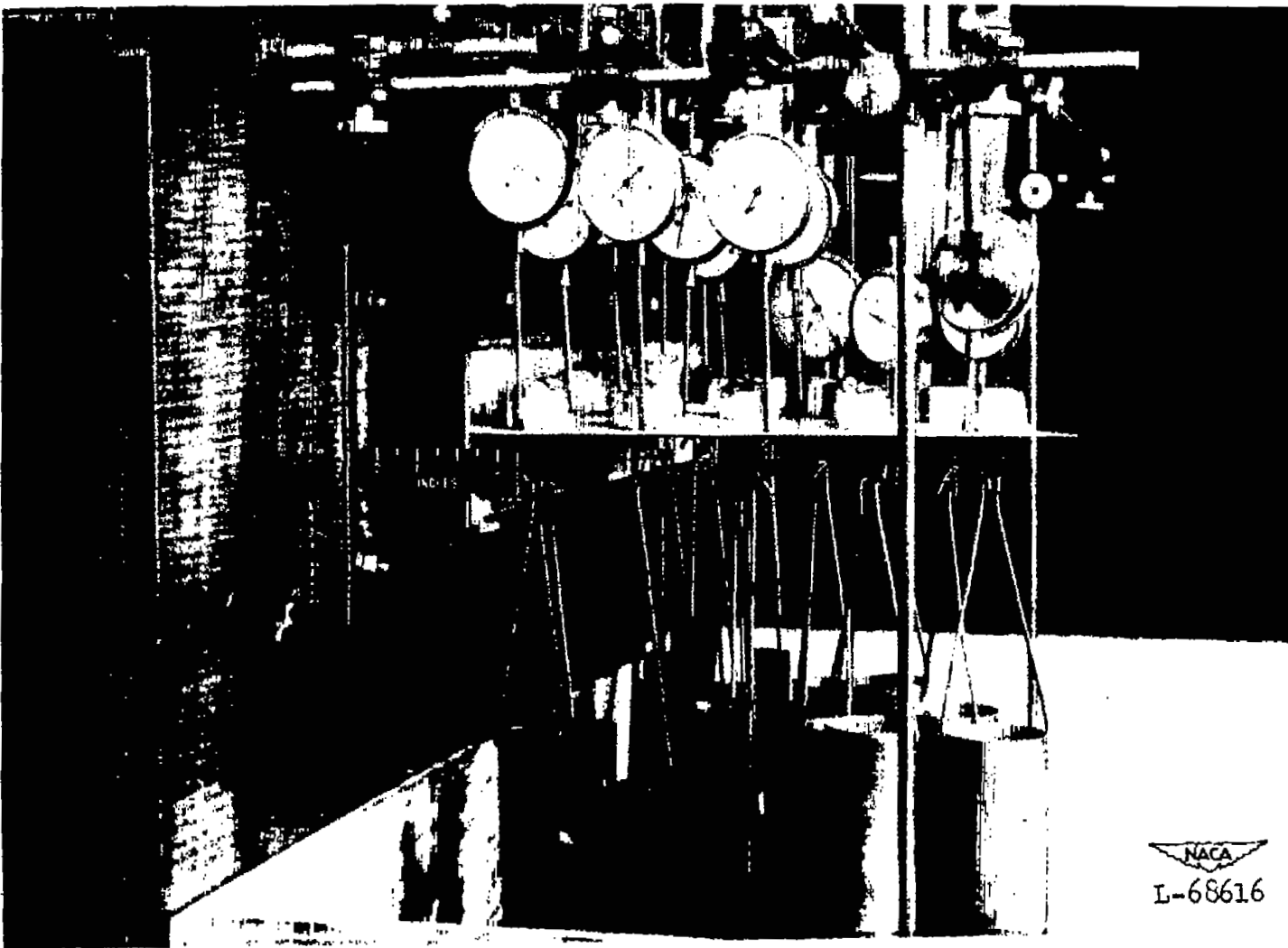


Figure 15.- A typical load test setup.

UNCLASSIFIED

~~CONFIDENTIAL~~